EasyChair Preprint

№ 5868

A Closed-Form Solution of Drop Test on an Elastic Bar: Benchmarking Force Response of the Restrained Bar to Impact

Adib Hamdani and Pankaj Pankaj

June 23, 2021

https://doi.org/10.31436/iiumej.vxxixx.xxxx

A CLOSED-FORM SOLUTION OF DROP TEST ON AN ELASTIC BAR: BENCHMARKING FORCE RESPONSE OF THE RESTRAINED BAR TO IMPACT

ADIB HAMDANI[1,2*], PANKAJ PANKAJ[2]

[1]*Department of Mechanical Engineering, International Islamic University Malaysia, Malaysia*
[2]*Institute for Bioengineering, The University of Edinburgh, Edinburgh, United Kingdom*

**Corresponding author: hadib@iium.edu.my*

(Received: Day Month Year; Accepted: Day Month Year; Published on-line: Day Month Year)

ABSTRACT: The behaviour of an elastic bar; restrained at one end and subjected to a rigid impactor at the other end is evaluated in this analytical work. In the original work on this problem, duration of impact is only considered up to four-times of the time taken by compressive stress wave to travel from end struck to the bottom support and back. The current work revisits the closed-form solution provided in the literature in terms of the set of first four compressive stresses, then formulates these terms in programming language. The code is then utilised to derive arbitrary number of higher-order stress intervals depending on mass ratio of the system to complete the whole impact process. Compressive stress at the end struck and its corresponding load are then formulated for each stress interval by the current and previous compressive stress formula; a process which provides force history at the end struck for the whole impact duration. Parametric study is then performed on the number of selected input parameters in the stress equations e.g. mass ratio, drop height (or initial velocity), elastic modulus and length of the elastic bar; revealing proportional relations to apparent output variables obtained from force history, namely number of intervals, initial compressive stress, pulse width, peak load and interval frequency. These proportionalities and their corresponding mathematical relations are useful in explaining and correlating respective output variable-parameter relationships obtained via experimental or numerical works. The closed-form solution provided in this work serves as a benchmark to numerical or experimental impact problems assuming homogeneous and isotropic bar behaving linear elastically.

KEY WORDS: *Elastic bar, Stress intervals, Force at end struck, Impact and Mathematical relations.*

1. INTRODUCTION

This paper considers the behaviour of an elastic bar, restrained at one end and subjected to an impact force exerted by an incoming rigid impactor at the other end. The treatment in this work is analytical and was first considered by [1]. However, their work was limited to the analytical treatment of mass ratio, α (ratio of the impacted bar to the rigid moving impactor - always less than unity) values between 1 and 1/6. When an elastic bar is struck, it undergoes a compression phase of collision followed by an elastic restitution of contact [2]. For the mass ratios considered by [1], the duration in which this happens is less than $4T$, where T is time taken for the compressive stress wave to travel from the end struck to the restrained support and back. Determination of the complete contact duration, termed as pulse duration or pulse width (t_{pulse}), depends on the mass ratio; more compressive wave terms are required as the mass ratio decreases. This work extends derivation procedure of a set of compressive stresses, s_n, $n = 0, 1, 2, 3 \ldots$ expressed by [1] to arbitrary number of stress interval, $n + 1$. The derived

expressions of compressive stress at end struck enables analytical evaluation of compressive impact load experienced by the bar's end struck to be evaluated.

The main objectives of this research are first to derive higher-order compressive stress terms. Expressions for up to the fourth term, s_3, are first derived to gain an insight into the analytical formulation briefly provided by [1]. Further higher-order terms, which depend on the mass ratio, are then derived using a symbolic maths code developed in MATLAB (R2016a, 1994-2018 The MathWorks, Inc.). The ultimate output expected from this work is to obtain the analytical compressive load response history at the impacted end of the bar for smaller mass ratios, which are useful as a benchmark closed- form solution in explaining physical phenomenon of axial bar impact as well as validating numerical finite element (FE) models. Then the study attempts to express relations between output variables from the obtained pulse and input parameters governing the axial impact problem.

2. PROBLEM DEFINITION

Consider a stationary elastic cylinder with diameter, 2r, and length, l, subjected to impact due to an incoming rigid impactor at one end (called the end struck), while the other end is fully-restrained as shown in Fig. 1as explained by [1]. The impactor has an initial velocity, v_0, just prior to the first contact at time $t = 0$. Mechanical impedance of a medium is defined as a product of the medium's elastic wave velocity and its mass density. Therefore, based on impedance components of bar's material, i.e. mass density (ρ) and elastic modulus (E); the initial compressive stress at impact time $t = 0$ is given by

$$\sigma_0 = v_0\sqrt{\rho E}, \qquad (1)$$

where $\sqrt{\rho E}$ is an alternative expression for the bar's impedance. Eq. (1) shows that initial stress σ_0 is dependent on the impactor's initial velocity, v_0. This initial stress expression is used repeatedly throughout the stress wave derivation process while applying the boundary condition between intervals. The first compressive stress wave, s0, originates from the equation of motion of the body and is only applicable for the first stress wave interval duration,

$$T = \frac{2l}{c}, \qquad (2)$$

where c is the elastic wave speed, governed by material's elastic properties i.e.

$$c = \sqrt{\frac{E}{\rho}}, \qquad (3)$$

for a one-dimensional problem.

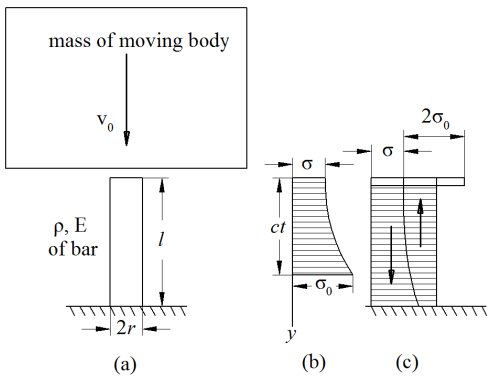

Fig. 1. (a) The system; (b) stress wave at $t < T/2$; and (c) stresses at $t = T$

https://doi.org/10.31436/iiumej.vxxixx.xxxx

Individual compressive wave terms required to evaluate the total stress at the end struck, $\sigma(t)$ are first derived for up to $t = 4T$. Time of contact or pulse duration can be estimated by

$$t_{\text{pulse}} \approx \frac{\pi l}{c}\sqrt{\frac{1}{\alpha}}, \qquad (4)$$

which works well for systems with very small mass ratio [1]. Considering normalised time $2\frac{t}{T} = 2, 4, 6, 8 \ldots$ corresponding to the first, second, third, fourth, . . . intervals respectively, the required number of intervals, N is estimated by using the normalised time of pulse width, i.e.

$$2N = 2\frac{t_{\text{pulse}}}{T}. \qquad (5)$$

Derivation of these sequential compressive stress waves, s_n, leads to total compressive stress history, $\sigma(t)$, at the impacted surface of the bar. The total compressive stress at end struck is calculated as the summation of compressive wave moving towards fixed end at current time, $s_n(t)$ and delayed moving wave at the previous time interval, $s_{n-1}(t-T)$ expressed as

$$\sigma_n(t) = s_n(t) + s_{n-1}(t-T). \qquad (6)$$

The total compressive stress in the history of the end struck is transformed to force history by multiplying the stress values with cross- sectional area (A) of the bar. In the case of drop test from a certain height, h, the initial velocity is given by

$$v_0 = \sqrt{2gh}; \qquad (7)$$

where g is the acceleration due to gravity. In this work, the effect of mass ratio (α), drop height (h), elastic modulus (E) and length of elastic bar (l) on the resulting output variables obtained from force history viz. number of intervals (N), initial compressive stress (σ_0), peak load (F_{max}), pulse width (t_{pulse}) and interval frequency (f) is considered.

3. FIRST COMPRESSIVE STRESS AND DERIVATION OF SUBSEQUENT INTERVALS

In this section, a set of first four compressive stress responses, s_n, $n = 0, 1, 2, 3$; are derived for stress wave history traversing to the base (fixed end) then returning back to the end struck for every sequential time interval. These resulting equations are cross-checked with final-form expressions in the referenced original work by [1].

The first compressive stress wave term, s_0, is obtained by using

$$s_0 = \sigma = \sigma_0 e^{-\frac{t\sqrt{E\rho}}{M}}, \qquad (8)$$

where M is the ratio of impactor's mass, m_{impactor} to the bar's impacted area, A [1], given by

$$M = \frac{m_{\text{impactor}}}{A}. \qquad (9)$$

Replacing

$$\frac{\sqrt{E\rho}}{M} = \frac{2\sigma}{T}, \qquad (10)$$

the expression for the first stress response becomes

$$s_0 = \sigma_0 e^{-\frac{2\alpha t}{T}}; \qquad 0 \le t \le T. \qquad (11)$$

Note that the mass ratio, α is expressed as

https://doi.org/10.31436/iiumej.vxxixx.xxxx

$$\alpha = \frac{\rho l}{M}, \qquad (12)$$

representing a dimensionless quantity.

In the subsequent compressive stress terms, they are represented by

$$s_n(t) = s_{n-1}(t-T) - \frac{4\alpha}{T} e^{-\frac{2\alpha t}{T}} \left[\int e^{\frac{2\alpha t}{T}} s_{n-1}(t-T)dt + C_n \right], \qquad (13)$$

where C_n is the constant of integration in the $(n+1)^{\text{th}}$ expression. The constant is found by applying boundary condition at the end of every interval, $t = (n+1)T$, at which the compressive stress at end struck suddenly increases by $2\sigma_0$ as shown in Fig. 1(c); a condition expressed as

$$[\sigma_{n-1}(t)]_{t=nT} + 2\sigma_0 = [\sigma_n(t)]_{t=nT}, n = 1, 2, 3, \ . \ . \ . \ ; \qquad (14)$$

where $\sigma_n(t)$ and $\sigma_{n-1}(t)$ are total stresses at instantaneous start of next and the end of previous intervals respectively. For instance, the conditions in Eq. (14) for the instantaneous starting time of second and third intervals are written as

$$s_0(t) + 2\sigma_0 = [s_1(t) + s_0(t-T)]_{t=T}, \qquad (15)$$

and

$$[s_1(t) + s_0(t-T)]_{t=2T} + 2\sigma_0 = [s_2(t) + s_1(t-T)]_{t=2T} \qquad (16)$$

respectively. After simplification, the compressive stress terms in Eq. (13) are expressed in a general form as

$$s_n(t) = s_{n-1} + \sigma_0 e^{-2\alpha\left(\frac{t}{T}-n\right)} \left[\sum_{m=0}^{n} k_m 4\alpha^m \left(n - \frac{t}{T}\right)^m \right]; \ nT \le t \le (n+1)T. \qquad (17)$$

Eq. (17) characterises all except s_0, in which constant $k_m, m = 0, 1, 2, 3, \ . \ . \ .$ are shown in Table 1 for the second (s_1) until the sixth stress intervals (s_5). Constants in the first three stress expressions in Table 1 match with the derivation by [1].

Table 1: Constant k_m in Eq. (17) for s_1 until s_5

s_n	m	k_m constant
s_1	0	1
	1	1
s_2	0	1
	1	2
	2	2
s_3	0	1
	1	3
	2	6
	3	8/3
s_4	0	1
	1	4
	2	12
	3	32/3
	4	8/3
s_5	0	1
	1	5
	2	20
	3	80/3
	4	40/3
	5	32/5(3)

As compressive stress expression in Eq. (17) becomes substantially long for $n > 3$, hence the problem is generalised in a programming language with the purpose of developing a symbolic code for arbitrary number of higher-order stress intervals. The procedure utilises 'symbolic math computation' in MATLAB which the results are validated against [1] in terms of the interval and total compressive stress for mass ratio of 1/8 as shown in Fig. 2. The input parameters are set for $\sigma_0 = 1$ in this example. The graphs demonstrate instantaneous rise of stress at the beginning of each interval ($2t/T = 2, 4, 6, \ldots$) and decaying stress values until the next interval as described by Eqs. (14-16) and (17) respectively. Fifty data points are assigned in each interval to plot graphs in Fig. 2.

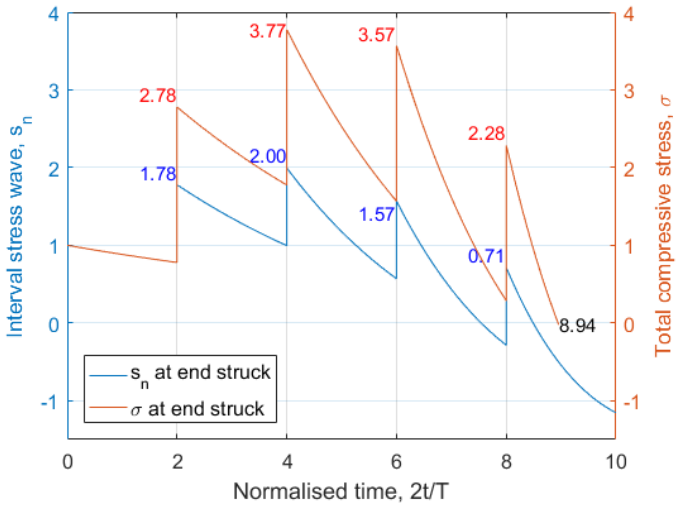

Fig. 2. Interval and total compressive stress for a system with mass ratio $\alpha = 1/8$. Stress unit is unnecessary.

Total compressive stress as a pulse response in Fig. 2 shows the compression phase of collision up to the peak stress, followed by restitution phase of contact post the peak point until the stress drops back to zero [2] during the fifth interval. Its stress values during instantaneous rise depicts summation of the current stress wave and the delayed wave of the previous time interval as described in Eq. (6). This $\sigma(t)$ pulse response exhibits unsymmetrical bell shaped curve overall, which becomes almost symmetrical if it constitutes a substantially high number of intervals corresponding to cases having small mass ratio values [3]. Furthermore, force response is obtained by diving the compressive stress history with the impacted cross-sectional area of the axial bar.

4. PARAMETRIC STUDY

The input parameters governing impulsive response are provided in the first stress wave, s_0 as shown in Eqs. (1, 8), such as mass ratio, initial velocity or drop height and elastic bar's material properties (E and ρ). The expression includes structural dimensions as well, which are cross-sectional area (A) and length of the bar (l); in the form of mass ratio (Eq. 9, 12) and interval time (Eq. 2). This section analyses the effect of these parameters on four main output variables from the system, namely number of stress intervals (N), maximum total stress or its corresponding peak load ($F_{\max}$), impact duration or pulse width (t_{pulse}) and interval frequency (f) which is an inverse of T.

4.1. Mass ratio, α

The mass ratio, α is a function of density and dimension of elastic bar, as well as the mass of rigid impactor (Eqs. 9, 12). The effect of mass ratio on stress values and number of intervals is

shown in Fig. 3 for interval stress wave and total compressive stress. These graphs of mass ratio ranging between one and one-sixth replicate plots by [1], hence proving the reliability of the developed code in this work to produce accurate stress response of this impact problem.

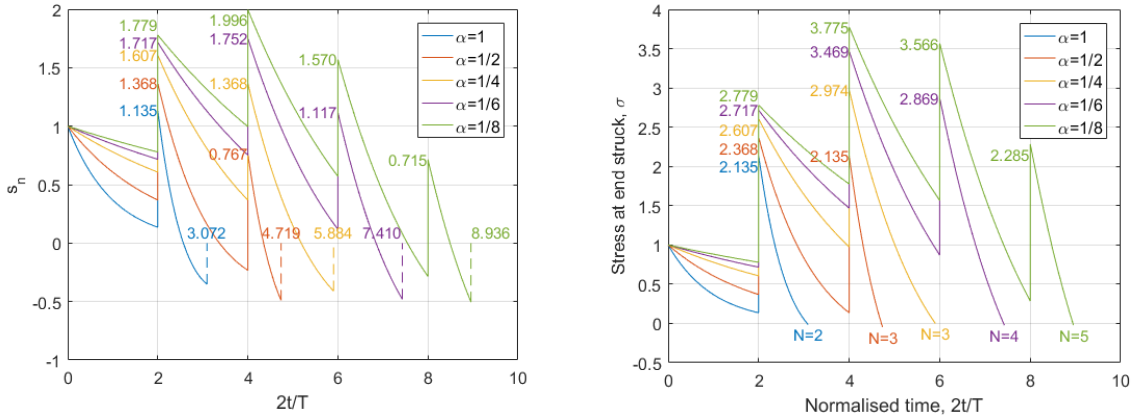

(a) Interval stress wave, s_n (b) Total compressive stress, $\sigma(t)$

Fig. 3. Effect of mass ratio on stresses and number of intervals. Units are consistent.

The end time or pulse width is determined by using linear interpolation of datapoints, estimating the corresponding time when stress value drops to zero. This interpolation method is accurate when the number of datapoints is sufficiently adequate in plotting the final stress interval. The required number of intervals, N can be estimated by

$$N = \frac{\pi}{2}\sqrt{\frac{1}{\alpha}}, \qquad (18)$$

as proposed by [1], approximated from pulse width duration in Eq. (4). Some discrepancies are observed between the estimator in Eq. (18) with the actual required N as shown in Fig. 3, understandably due to α being relatively close to unity; this estimation improves as mass ratio is sufficiently small. Practically, it is advised to consider one higher interval expression to accommodate whole pulse duration in the response.

4.2. Drop height, *h*

Parametric study on drop height, h is based on a report by [3], in which trabecular bone samples having diameter of 10.6 mm and length of 12 mm were impacted by a 26-g hammer as shown in Table 2. The drop height corresponds to initial velocity, v_0 by applying the principle of energy conversion as shown in Eq. (7). Trabecular bone's elastic modulus of 531 MPa is estimated by [4] and falls within ranges reported by many studies including [5-10].

Table 2: Summary on the effect of drop height parameter; Units: length [mm], mass [g], time [msec], elastic modulus [MPa], load [kN]

h [mm]	Input parameters				Output variables			
	v_0	$m_{impactor}$	E	ρ	F_{max}	N	t_{pulse}	f
100	1.40	26.62	531	1.31×10^{-3}	0.545	7	0.253	26.53
50	0.99				0.385			
25	0.7				0.272			
10	0.44				0.172			

https://doi.org/10.31436/iiumej.vxxixx.xxxx

The effect of drop height on the resulting force pulse is shown in Fig. 4, highlighting its effect on the force values in particular the peak force, F_{max} . Proportionality relation was found between F_{max} and $\sqrt{h}$ which supports the peak load-hip impact velocity relation found by [11]; a simulation work on sideways fall.

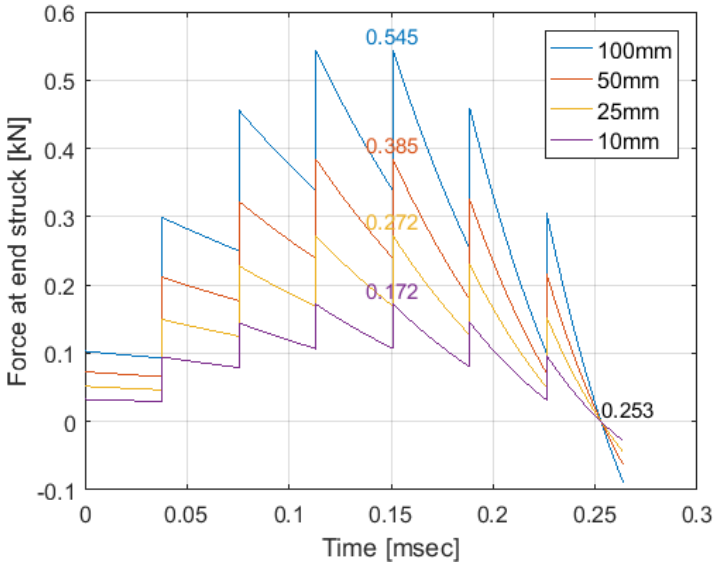

Fig. 4. Drop height effect on the peak load.

It is observed in Fig. 4 that interval time is unaffected by the change in drop height, so as its corresponding frequency, the number of stress intervals and the pulse width. These results are consistent with relations shown in Eqs. (2-4) and tabulated in Table 2.

4.3. Elastic modulus, *E* of the bar's material

Based on experimental work in [3], input parameters in this study of elastic modulus are defined as in Table 3, in which a 2.5-kg rigid impactor was dropped from 50 mm height on trabecular bone samples having average diameter of 10.6 mm and length of 21 mm. The material stiffness i.e. elastic modulus was revealed to affect all output variables except the number of stress intervals, *N*.

Table 3: Summary on the effect of elastic modulus parameter; Units: length [mm], mass [kg], time [msec], load [kN]

E [MPa]	Input parameters			Output variables			
	h	$m_{impactor}$	ρ	F_{max}	t_{pulse}	f	N
531	50	2.5	1.31×10^{-6}	2.41	3.30	15.19	50
400				2.09	3.80	13.19	
300				1.81	4.39	11.40	
200				1.48	5.37	9.30	
100				1.05	7.60	6.59	

Fig. 5(a) shows stiffer force response of bars with higher elastic modulus; an effect demonstrated by pulses having greater peak load at the expense of shorter pulse width. Fast Fourier transform is performed on the pulse, in which the process returns its interval frequency as shown in Fig. 5(b); indicating direct proportionality with the elastic modulus.

https://doi.org/10.31436/iiumej.vxxixx.xxxx

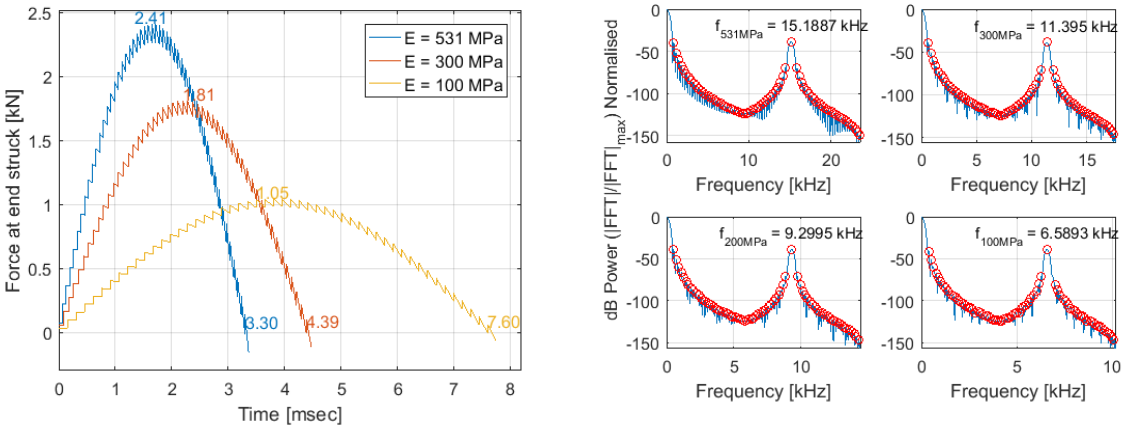

(a) On F_{max} and t_{pulse} (b) On f

Fig. 5. Bar's elastic modulus (E) effect.

The actual proportionality between some output variables and elastic modulus is shown in Fig. 6. Peak load is directly proportional to the square-root of elastic modulus, while pulse width is inversely proportional to that input as presented in Figs. 6(a) and 6(b) respectively; the results are consistent with observation on Eqs. (1, 4, 6, 11, 17). Hence, $t_{pulse} - \sqrt{E}$ relations can be derived via two methods: 1) by analytical method from the graph plots; and 2) by using Eq. (4) which is an estimation. Likewise, interval frequency is proportional to the surd of elastic modulus as suggested in Eqs. (2-3) and supported by returned frequency in Fig. 5(b).

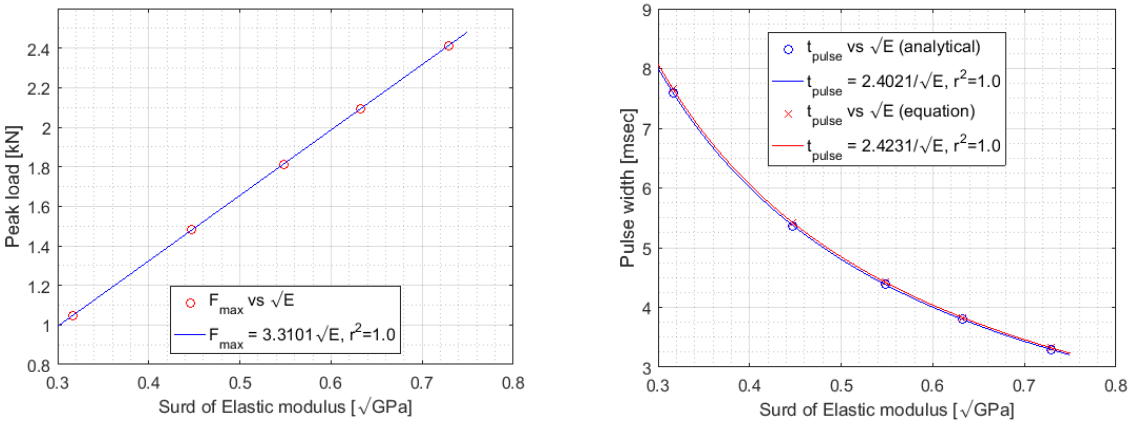

(a) Linear model of $F_{max} - \sqrt{E}$ (b) Power law (nonlinear inverse) model of $t_{pulse} - \sqrt{E}$

Fig. 6. Regression models relating output variables and $\sqrt{E}$.

Another output variable which can be estimated from the force response is the loading rate ($\dot{F}$) of the initial stage of the compression phase of collision [2], by taking the apparent gradient of the rising force response as shown in Fig. 7(a). In the current impact models, taking half of the curve's initial data in this compression phase gives the best linear fittings. Linear relation is revealed between $\dot{F}$ and E as shown in Fig. 7(b), which is very useful in analysing experimental results as force response is commonly measured in such laboratory work, such as in [3]. By relating the theoretical derivations in this parametric study with output variable-input parameter relations

https://doi.org/10.31436/iiumej.vxxixx.xxxx

obtained experimentally, researchers can benchmark their findings and perhaps create mathematical relations via both experimental and analytical works.

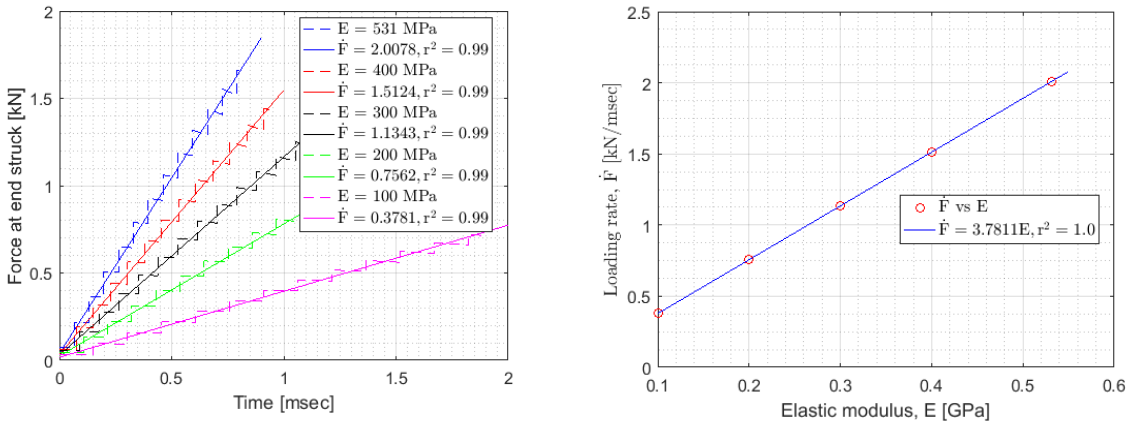

(a) Linear regression on half of the curve's initial data

(b) $\dot{F} - E$ relation

Fig. 7. Bar's elastic modulus effect on the loading rate, $\dot{F}$.

4.4 Length, *l* of the bar

This parametric study of length has similar definitions as in elastic modulus in the previous section, except that the modulus is kept at 531 MPa while the length is varied between 21 and 50 mm as tabulated in Table 4.

Table 4: Summary on the effect of length parameter. $m + 1$ is the interval in which the peak load is located; Basic units: length [mm], mass [kg], time [msec]

l [mm]	Input parameters				Output variables			
	h	$m_{impactor}$	E	ρ	F_{max}	t_{pulse}	f	N($m+1$)
21	50	2.5	0.531	1.31×10^{-6}	2.412	3.296	15.19	50(26th)
32					1.967	4.088	9.91	41(21st)
35					1.884	4.264	9.10	39(21st)
40					1.768	4.588	7.98	37(19th)
50					1.588	5.119	6.39	33(17th)

The length of elastic bar is a component of its structural stiffness and is inversely proportional to it. Hence, the effect of bar to the pulse response is expected to be the opposite of material stiffness (Fig. 5a), as shown in Fig. 8(a). Similar trend is shown for the returned interval frequency via fast Fourier transform method as depicted in Fig. 8(b). As length is one of parameters having direct proportionality with the mass ratio as stated in Eq. (12), therefore the effect of length is expected to be similar as in Fig. 3(b), and opposite to the interval frequency as shown in Fig. 8(b).

https://doi.org/10.31436/iiumej.vxxixx.xxxx

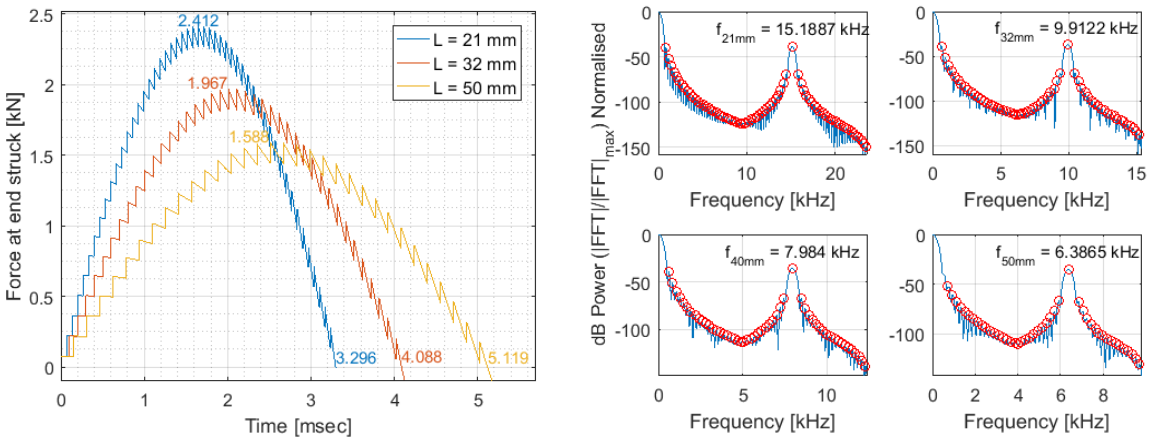

(a) On F_{max} and t_{pulse} (b) On f

Fig. 8. Bar's length (l) effect.

In establishing relation between peak load and the bar's length, there is no exact mathematical expression can be fitted for the data, as shown in Fig. 9; in which two power law relations are attempted together with a two-term exponential model to be the best regression models. However, under close scrutiny, the power law models maybe closely represented as $F_{max} \propto 1/\sqrt{l}$.

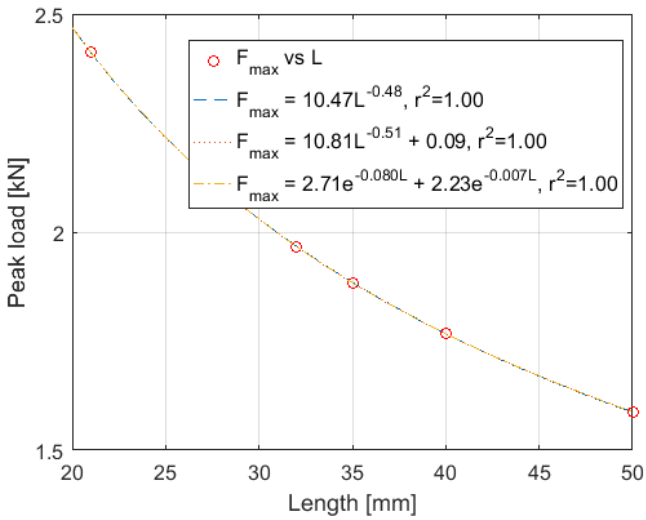

Fig. 9. Nonlinear regression models of $F_{\max} - l$ (Power laws and exponential).

Pulse width is found to have direct proportionality with square-root of length i.e. $t_{pulse} \propto \sqrt{l}$ based on both obtained pulses and predictor equation. On the other hand, frequency establishes inverse relation with the length, which has the opposite effect to the pulse width or total impact time. These effects are shown in Figs. 10(a) and 10(b) respectively.

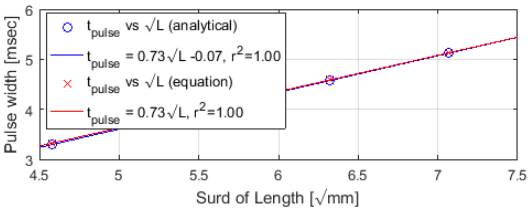

(a) Linear models of $t_{pulse} - \sqrt{l}$

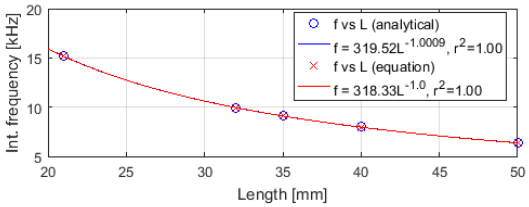

(b) Power law models of $f - 1/l$

Fig. 10. Regression models relating pulse width and interval frequency with length.

5. SUMMARY

This work revisits the axial bar impact problem briefly explained by [1] and subsequently derive the compressive stress expressions in MATLAB programming language up to arbitrary number of intervals. Parametric analysis is conducted on the resulting developed stress equations, hence highlighting some important relations between output variables and input parameters; most notably $F_{\max} \propto \sqrt{E}$, $t_{\text{pulse}} \propto 1/\sqrt{E}$ and $\dot{F} \propto E$. Such relations serve as benchmark to validate experimental or numerical work and may also be used to derive mathematical relations explaining how certain parameters are related to their corresponding outcomes [3].

ACKNOWLEDGEMENT

The first author is indebted to the Ministry of Education, Malaysia for the award of PhD sponsorship.

REFERENCES

[1] Timoshenko S, Goodier JN. (1951) Theory of Elasticity, 2nd Ed. McGraw-Hill Book Company, Inc., New York.
[2] Stronge WJ. (2000) Impact Mechanics, Cambridge University Press.
[3] Rosli AHB. (2019) Characterisation of Trabecular Bone Behaviour under Impact, PhD Thesis, The University of Edinburgh.
[4] Xie S, Wallace RJ, Callanan A, Pankaj P. (2018) From Tension to Compression: Asymmetric Mechanical Behaviour of Trabecular Bone's Organic Phase. Annals of Biomedical Engineering, 46(6):801-809.
[5] Lotz JC, Gerhart TN, Hayes WC. (1990) Mechanical Properties of Trabecular Bone from the Proximal Femur: A Quantitative CT Study. Journal of Computer Assisted Tomography, 14(1):107-114.
[6] Keller TS. (1994) Predicting the Compressive Mechanical Behaviour of Bone. Journal of Biomechanics, 27(9):1159-1168.
[7] Goulet RW, Goldstein SA, Ciarelli MJ, Kuhn JL, Brown MB, Feldkamp LA. (1994) The Relationship between the Structural and Orthogonal Compressive Properties of Trabecular Bone. Journal of Biomechanics, 27(4):375-389.
[8] Li B, Aspden RM. (1997) Composition and Mechanical Properties of Cancellous Bone from the Femoral Head of Patients with Osteoporosis or Osteoarthritis. Journal of Bone Mineral Research, 12(4):450-456.
[9] Ciarelli TE, Fyhrie DP, Schaffler MB, Goldstein SA. (2000) Variations in Three-dimensional Cancellous Bone Architecture of the Proximal Femur in Female Hip Fractures and in Controls. Journal of Bone and Mineral Research, 15(1):32-40.

[10] Kaneko TS, Bell JS, Pejcic MR, Tehranzadeh J, Keyak JH. (2004) Mechanical Properties, Density and Quantitative CT Scan Data of Trabecular Bone with and without Metastases. Journal of Biomechanics, 37(4):523-530.
[11] Majumder S, Roychowdhury A, Pal S. (2008) Effects of Trochanteric Soft Tissue Thickness and Hip Impact Velocity on Hip Fracture in Sideways Fall Through 3D Finite Element Simulations. Journal of Biomechanics, 41(13):2834-2842.